

Planar Lightwave Integrated Circuits With Embedded Actives for Board and Substrate Level Optical Signal Distribution

Nan M. Jokerst, *Fellow, IEEE*, Thomas K. Gaylord, *Fellow, IEEE*, E. Glytsis, *Senior Member, IEEE*, Martin A. Brooke, *Member, IEEE*, S. Cho, *Member, IEEE*, T. Nonaka, T. Suzuki, Demetris L. Geddis, *Member, IEEE*, Jaemin Shin, R. Villalaz, J. Hall, Ananthasayanam Chellapa, and M. Vrazel

Abstract—As the data rate of integrated circuits dramatically increases, interconnection speed at the backplane and board levels are beginning to limit system performance, which drives investigations into alternative interconnection technologies. Critical factors to consider when evaluating alternative interconnection approaches include interconnect speed, power consumption, area, and compatibility with current backplane and board integration technologies. Optical interconnections can achieve very high speed with a significant reduction in interconnect footprint compared to transmission lines, robust signal quality in high-density interconnection systems because of immunity to electromagnetic interference, and potentially simple to design (compared to transmission lines) lines with materials which can be postprocessed onto printed wiring boards or integrated into the board structure. This paper explores design options for planar optical interconnections integrated onto boards, discusses fabrication options for both beam turning and embedded interconnections to optoelectronic devices, describes integration processes for creating embedded planar optical interconnections, and discusses measurement results for a number of integration schemes that have been demonstrated by the authors. In the area of optical interconnections with beams coupled to and from the board, the topics covered include integrated metal-coated polymer mirrors and volume holographic gratings for optical beam turning perpendicular to the board. Optical interconnections that utilize active thin film (approximately 1-5 μm thick) optoelectronic components embedded in the board are also discussed, using both Si and high temperature FR-4 substrates. Both direct and evanescent coupling of optical signals into and out of the waveguide are discussed using embedded optical lasers and photodetectors.

I. INTRODUCTION

AS the data rate of integrated circuits dramatically increases, interconnection speed at the backplane and board levels are beginning to limit system performance, which drives investigations into alternative interconnection technologies. Critical factors to consider when evaluating alternative in-

terconnection approaches include interconnect speed, power consumption, area, and compatibility with current backplane and board integration technologies. Optical interconnections can achieve very high speed with a significant reduction in interconnect footprint compared to transmission lines, robust signal quality in high density interconnection systems because of immunity to electromagnetic interference, and potentially simple to design (compared to transmission lines) lines with materials which can be postprocessed onto printed wiring boards or integrated into the board structure.

These advantages of optical interconnections have generated a high level of research interest in the area of planar optical interconnections that can be integrated, in a miniaturized format, at the board level. The integration technologies for implementing these optical interconnections at the board level are methods for the integration of optical signals and optoelectronic devices in a system-on-a-package (SOP) format. These embedded SOP optical interconnections are usually in a waveguide format at the board level, and can utilize either embedded thin-film optoelectronic devices or can use bump bonded optoelectronic devices with beam turning elements for E/O and O/E conversion.

This paper explores design options for planar optical interconnections integrated onto boards, discusses fabrication options for both beam turning and embedded interconnections to optoelectronic devices, describes integration processes for creating embedded planar optical interconnections, and discusses measurement results for a number of integration schemes that have been demonstrated by the authors. In the area of optical interconnections with beams coupled to and from the board, the topics covered include integrated metal-coated polymer mirrors and volume holographic gratings for optical beam turning perpendicular to the board. Optical interconnections that utilize active thin-film (approximately 1-5 μm thick) optoelectronic components embedded in the board are also discussed, using both Si and high temperature FR-4 substrates. Both direct and evanescent coupling of optical signals from the waveguide using embedded optical photodetectors (PDs) are also discussed herein. Optical coupling from thin-film edge-emitting lasers integrated with planar waveguides has also been recently reported.

II. OPTICAL INTERCONNECTIONS IN ELECTRICAL SYSTEMS

Many quantitative comparisons of interconnection performance have been published discussing electrical and optical interconnections [1]–[3], and the topology and processes for

Manuscript received January 25, 2004; revised April 23, 2004. This work was supported by the National Science Foundation Electronic Packaging Research Center and its Member Companies.

N. M. Jokerst and S. Cho are with the Department of Electrical Engineering, Duke University, Durham, NC 27706 USA (e-mail: njokerst@ee.duke.edu).

T. K. Gaylord, E. Glytsis, M. A. Brooke, T. Suzuki, J. Shin, R. Villalaz, J. Hall, A. Chellapa, and M. Vrazel are with the Georgia Institute of Technology, Atlanta, GA 30332 USA.

T. Nonaka is with Toray Industries, Tokyo 103-8666, Japan (e-mail: Toshihisa_Nonaka@nts.toray.co.jp).

D. L. Geddis is with the Department of Engineering, Norfolk State University, Norfolk, VA 23504 USA (e-mail: dgeddis@nsu.edu).

Digital Object Identifier 10.1109/TADVP.2004.831894

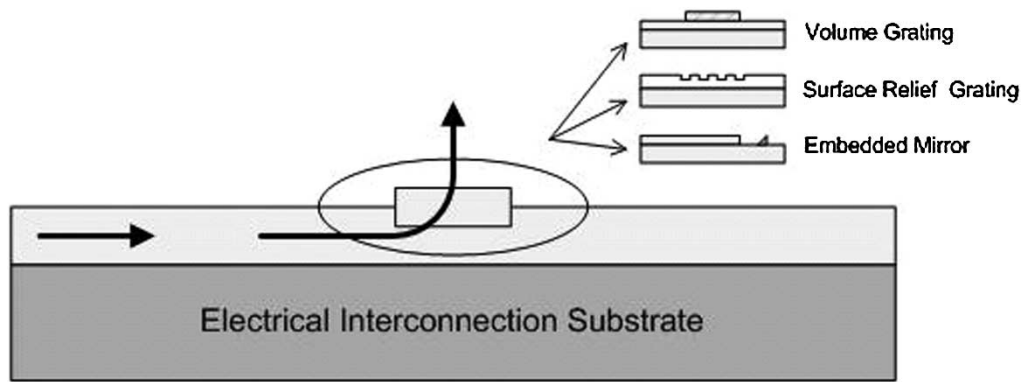


Fig. 1. Embedded optical interconnection beam turning options.

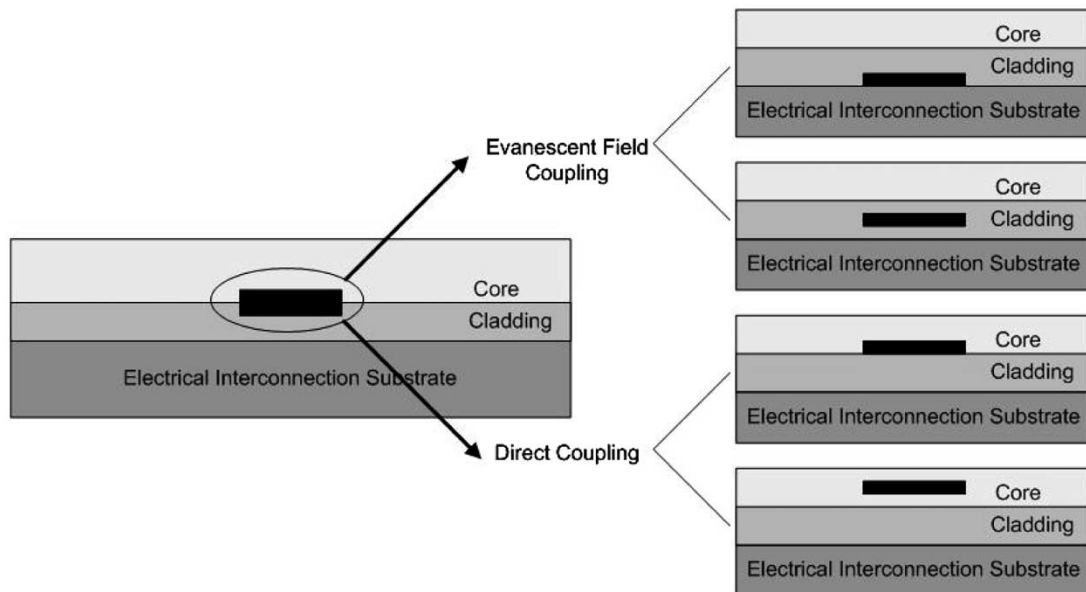


Fig. 2. Active thin-film optoelectronic device options for embedded optical interconnections.

the integration of optical interconnections into an electrical interconnection system is a topic of current research interest. Current optical interconnect approaches include free space interconnects with diffractive optical elements [4], silicon optical bench interconnects [5], and guided wave interconnections, including substrate guided mode interconnects [6], fiber optic waveguides [7], and integrated waveguides [8]. This paper focuses upon planar optical interconnections that are integrated directly onto electrical interconnection substrates for backplane and board-level applications.

High-speed electrical interconnection systems are essentially planar, with perpendicular connections often realized in either a daughter board/backplane or flex format. Thus, planar waveguide optical interconnection schemes match the electrical systems from a topographical standpoint, in that both planar optical interconnections and perpendicular optical interconnections are feasible in integrated systems. These two basic functions, planar guided wave optical interconnections and optical beam turning perpendicular to the plane of the substrate, can be utilized in a variety of formats, including interfaces to fibers, lasers, modulators, and PDs, the latter three serving as transducers to the electrical system. Thus, integrated optical interconnection tech-

nology is quite versatile in implementation, and a large “tool kit” of optical beam manipulation and optical function [splitters, wavelength division multiplexing (WDM) and spatial multiplexing] options can be implemented in, and perpendicular to, the substrate plane.

There is a variety of approaches to the partitioning of optical and electrical signals in the plane (on the board) in an integrated electrical/optical interconnection system. Figs. 1 and 2 illustrate two of the basic partitioning options: (Fig. 1) turn the optical beam out of the substrate into the optoelectronic active device; or (Fig. 2) confine the optical beam as a guided wave in the substrate, and embed the active optoelectronic devices in the substrate. There are many options for turning optical beams, some of which are shown schematically in Fig. 1. Optical beams can be turned 90 degree using 45 degree mirrors or gratings, and can be turned into either optical/optoelectronic devices, or onto optoelectronic integrated circuits (OEICs), which may contain a combination of active and passive optical/optoelectronic devices and circuitry. By employing diffractive optical elements, such as preferential volume gratings, high coupling efficiency and limited spectral selectivity can be achieved [9], with some scattering loss. Mirrors are attractive for highly multimoded signals, whereas gratings

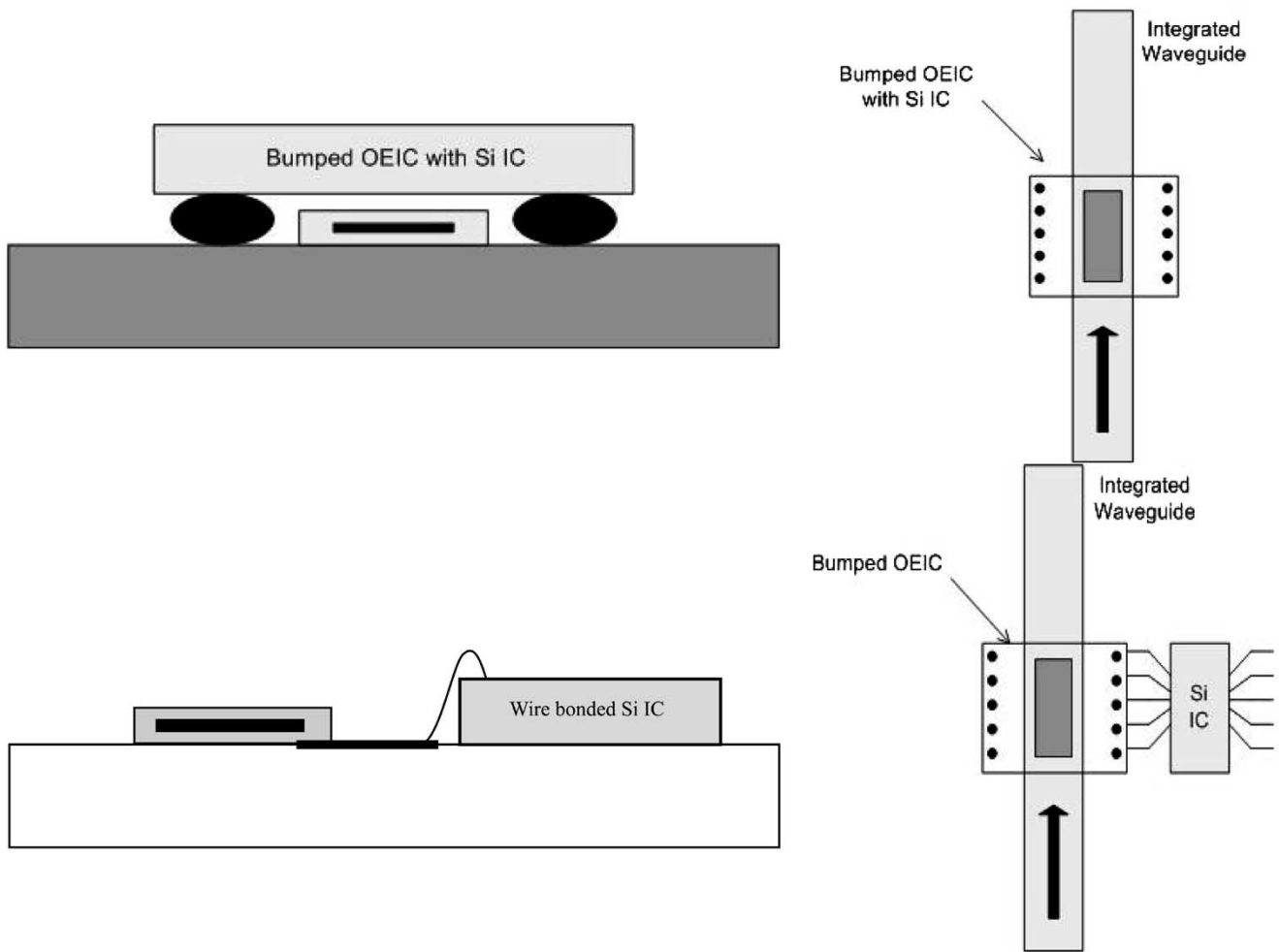


Fig. 3. Circuit interconnection options for embedded optical interconnections. Note that the top figure can use either a beam turning element or a thin-film active optoelectronic device embedded in the waveguide. The bottom figure, illustrating wire bonding, can only be used with a thin-film active optoelectronic device embedded in the waveguide.

are attractive for signals with one or few modes. To emit or detect this perpendicularly outcoupled beam means that the active optoelectronic device must operate facing the board/module/chip, in a flip chip orientation or as a flip chip OEIC [10], as shown in Fig. 3. Optical alignment design considerations become increasingly important with increasing speed since PDs decrease in size and responsivity with increasing data rates.

An alternative approach is to have the optical signals originate and/or terminate in the waveguide directly on the board, without optical beam turning. Fig. 2 illustrates some of the options for embedding a detector in a waveguide, including embedding in the core (for direct coupling, as indicated in Fig. 2), and in the cladding (for evanescent coupling, also as indicated in Fig. 2). Optical interconnections with integrated waveguides and OE devices in the substrate and epilayers [11]–[15] have been reported in semiconductors, with high coupling efficiency and monolithic integration. However, the use of polymer waveguides and low cost epoxy and polymer substrates is particularly interesting for optical interconnections in traditional epoxy electrical interconnection substrates. Thus, polymer waveguides for low cost optical interconnections that are process compatible with current board, module, and integrated circuit technology is a research goal. Polymer waveguides integrated onto Si [14] or GaAs [15] electrical interconnection substrates that have PDs

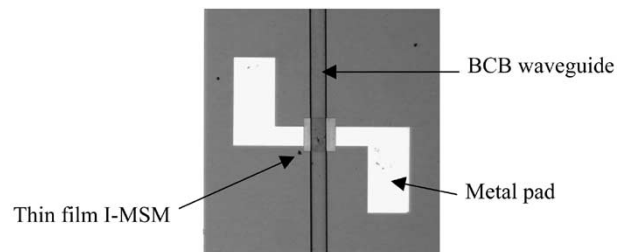


Fig. 4. Thin-film I-MSM PD bonded to metal pads on a SiO_2/Si substrate with a BCB polymer waveguide embedding the thin-film PD.

fabricated in the substrate have been demonstrated, but this approach does not enable the use of epoxy boards. However, heterogeneously integrated thin-film active optoelectronic (OE) devices embedded in waveguides can be bonded to metal pads deposited onto any host substrate, including polymer and epoxy boards such as FR-4. Polymer waveguide material can then subsequently be deposited directly onto the thin-film active OE devices to embed them in the waveguide, as illustrated in Fig. 2. The electrical integrated circuit interconnection to the OE device pads can then be implemented using either bump bonding, as shown in Fig. 3, or through wire bonding, as illustrated in Fig. 4.

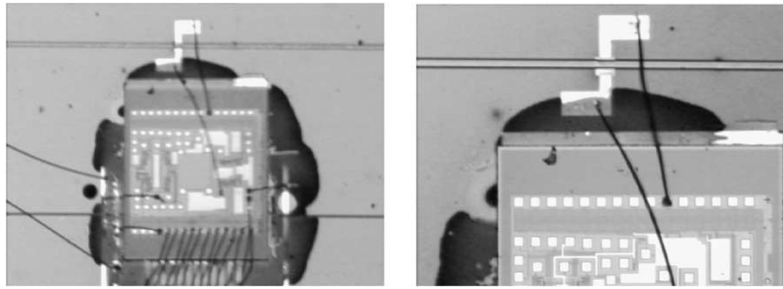


Fig. 5. Photomicrographs of a thin-film I-MSM PD embedded in a BCB waveguide, with the PD/BCB structure integrated onto a SiO_2/Si substrate. The optical signal is coupled from the waveguide to the embedded PD. The PD output signal serves as the input to the TIA that is wire bonded to the PD pads. The right hand photomicrograph is a close up view of the photomicrograph at left.

The heterogeneously integrated thin-film OE devices embedded in waveguides enables the interconnect designer the option to create an optical interconnection on the board that has exclusively electrical inputs and/or outputs, thus mimicking an electrical interconnection substrate. Thin-film InGaAsP multiple-quantum-well edge-emitting lasers integrated onto SiO_2/Si substrates have been reported, and these lasers have been launched into polymer waveguides [16]. The embedded thin-film OE device integration scheme reduces waveguide to active OE device optical alignment to an assembly step with sequentially aligned masking steps, which mimics integrated circuit fabrication. Thus, the optically emitted or detected beam is aligned to the waveguide through photolithography, not through the alignment of an optical turning device. In addition, since the thin-film OE devices are embedded in the waveguide, there is no air gap between the OE device and the waveguide. Alternatively, for beam turning, vertical-cavity surface-emitting lasers (VCSELs) can be used, which emit vertically (upward or downward). VCSELs have also been reported in thin-film format for heterogeneous integration [17]. Finally, for advanced optical signal distribution and processing, the integration of additional planar lightwave circuit passive and active embedded devices enables functions such as multiplexing, wavelength conversion, gain, and parametric processing. To minimize the impact of introducing optical interconnections into electrical interconnection substrates, the embedded waveguide interconnections can be integrated onto a fabricated electrical interconnection substrate through postprocessing. To enhance yield, at the board/module level, the optical interconnections can be electrically tested before chipset integration.

This paper will explore embedded optical interconnection technology through both heterogeneously integrated thin-film active optoelectronic devices, as well as the implementation of integrated beam turning options that include epoxy micromirrors and integrated diffraction gratings. Section III discusses embedded thin-film active OE devices integrated onto Si and high-temperature FR-4, Section IV explores integrated optical beam turning devices (micromirrors and gratings), and Section V summarizes the paper.

III. PLANAR OPTICAL INTERCONNECTIONS USING EMBEDDED THIN-FILM ACTIVE OPTOELECTRONIC DEVICES IN WAVEGUIDES

A. Embedded Thin-Film PDs in Polymer Waveguides on Si

To embed a thin-film active OE device in a polymer waveguide, as illustrated in Fig. 2, the OE device fabrication and the

waveguide fabrication must be cooptimized. This paper will explore embedded thin-film InGaAs PDs, bonded to Si/SiO_2 substrates that are subsequently embedded in a spin-coated polymer waveguide structure, and tested. These PDs embedded in waveguides were also tested by wire bonding commercial Maxim transimpedance amplifiers (TIAs) to the PD output pads.

The integrated structures tested were thin-film inverted metal-semiconductor-metal (I-MSM) PDs embedded in a waveguide integrated onto Ti/Au pads on Si/SiO_2 ($3\ \mu\text{m}$ thick) substrates, which had a BCB (core waveguide layer) spin coated onto the PDs. The $3\text{-}\mu\text{m}$ -thick SiO_2 layer acts as a cladding and buffer layer for the BCB waveguide. Contact pads of Ti/Au ($400\ \text{\AA}/5000\ \text{\AA}$) were deposited and patterned on this substrate. Next, the thin-film PDs were independently grown and fabricated, and bonded (metal PD pad to metal pad on Si) to the Si substrate. The as-grown MSM material was InP/InGaAs (stop etch layer)/ $\text{Al}_{0.48}\text{In}_{0.52}\text{As}$ cap layer ($400\ \text{\AA}$)/ $\text{Al}_{0.48}\text{In}_{0.52}\text{As}$ graded to $\text{In}_{0.53}\text{Ga}_{0.47}\text{As}$ ($600\ \text{\AA}$)/ $\text{In}_{0.53}\text{Ga}_{0.47}\text{As}$ ($0.74\text{-}\mu\text{m}$ -thick absorbing layer)/ $\text{In}_{0.53}\text{Ga}_{0.47}\text{As}$ graded to $\text{Al}_{0.48}\text{In}_{0.52}\text{As}$ ($600\ \text{\AA}$)/ $\text{Al}_{0.48}\text{In}_{0.52}\text{As}$ cap layer ($400\ \text{\AA}$). Schottky contacts of $40\ \text{\AA}\ \text{Pt}/350\ \text{\AA}\ \text{Ti}/400\ \text{\AA}\ \text{Pt}/2500\ \text{\AA}\ \text{Au}$ were deposited, and interdigitated fingers $100\ \mu\text{m}$ long with $2\ \mu\text{m}$ finger width and $2\ \mu\text{m}$ finger spacing were patterned on a $100\ \mu\text{m} \times 150\ \mu\text{m}$ absorbing area. The $400\text{-}\text{\AA}$ -thick Pt layer acts as a diffusion barrier to the Au during the polymer waveguide thermal curing process [18], [19]. Finally, after the thin-film I-MSMs were bonded to the metal pads on the SiO_2/Si , $2.7\ \mu\text{m}$ of Benzocyclobutene (BCB) core layer was spin coated onto the PD/Si sample and cured at $240\ ^\circ\text{C}$ for 1 h.

The thin-film PD is bonded to metal pads on the SiO_2 -coated Si substrate using a metal/metal bond. The I-MSM PD metalization constitutes one side of the metal/metal bond, and the pad on the substrate is the other side of the metal/metal bond. These metal/metal bonds are electrically conductive and mechanically stable bonds. Lifetime tests (5000 h) have been performed on thin-film LEDs bonded to silicon nitride-coated Si substrates using this metal/metal technology, showing that both the thin-film device and the bonds are reliable under these conditions [20]. Thermal cycling tests (5000 cycles) of thin-film PDs embedded in polymer waveguides integrated onto high temperature FR-4 have also been completed recently, with the thin-film devices operational throughout the testing (these results will be reported shortly) [21].

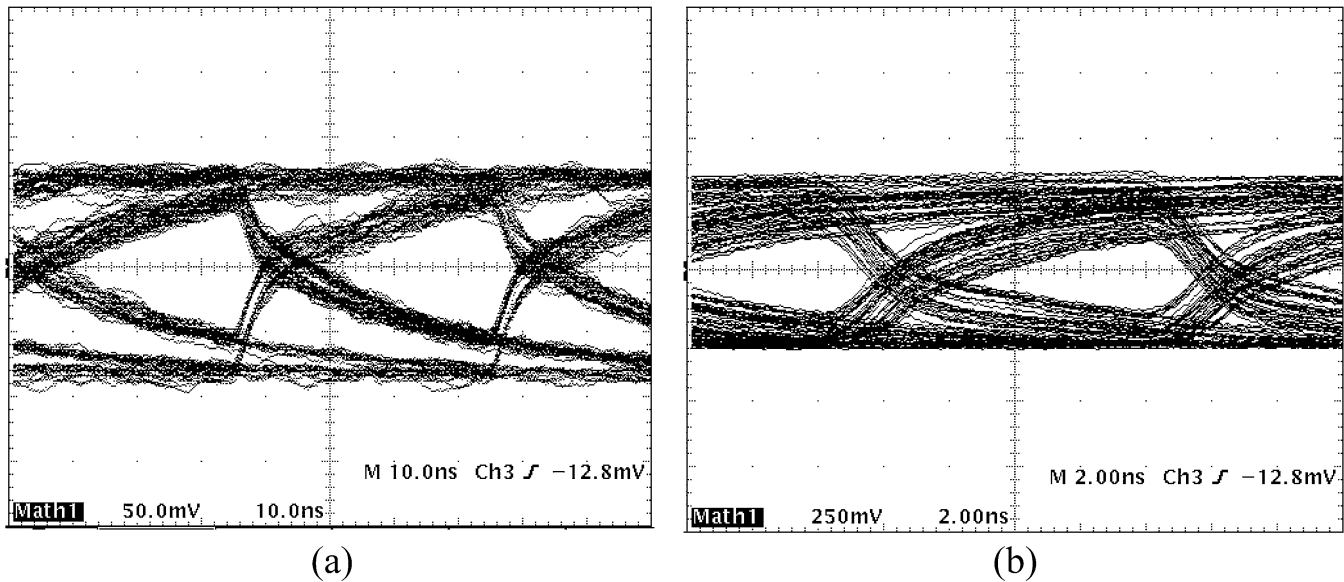


Fig. 6. Measured eye diagram. (a) 25 Mbps. (b) 100 Mbps.

To complete the waveguide integration process, the slab waveguide was patterned and etched into a $100\text{-}\mu\text{m}$ -wide channel using a photoresist mask and dry etching. The width of the fabricated waveguide matched the detection area of the embedded PD to maximize the coupling efficiency from the waveguide to the embedded PD [22]. Thus, carriers photogenerated by direct coupling from the waveguide into the PD are effectively swept into the interdigitated finger contacts. Fig. 4 is a photomicrograph of an I-MSM PD embedded in a BCB polymer waveguide on a SiO_2/Si substrate.

These embedded thin-film I-MSM PDs were also integrated with a TIA for testing. To test the PD on the integration substrate, a Maxim TIA was bonded to the SiO_2/Si substrate with epoxy, as shown in the photomicrograph in Fig. 5. The input to the TIA was then wire bonded to the pads to which the embedded PD was also bonded, as shown in Fig. 4. The entire SiO_2/Si substrate was then bonded to an FR-4 testboard with epoxy, as shown in Fig. 5. The signal and bias lines were then wirebonded to the FR-4 testboard. The long wirebonds have little effect on the performance of this structure, however, flip chip bonding of the circuit to the board (on top of the PD) will be necessary to reduce the electrical interconnection parasitics at high speeds (over 10 Gbps).

B. Experimental Characterization of PDs Embedded in Polymer Waveguides

The propagation loss of a BCB polymer waveguide (separately fabricated from those shown in Figs. 4 and 5) was measured using an optical fiber scanning method. The probing large core multimode fiber (core diameter = $600\text{ }\mu\text{m}$, $\text{NA} = 0.37$) measures the scattered optical signal from the channel waveguide. Using this method, the estimated propagation loss of the BCB polymer channel waveguide was 0.36 dB/cm at a wavelength of $1.3\text{ }\mu\text{m}$. This estimate includes intrinsic material, structural, and other propagation loss sources for the BCB waveguide, which is consistent with other reported results for BCB waveguides [23], [24].

Numerous BCB/PD/ SiO_2/Si structures have been characterized in terms of dark current and coupling efficiency. This embedded structure can be tuned to increase or decrease the coupling efficiency based upon the size of the PD and the waveguide, as well as the position of the PD in the integrated waveguide structure. As an example, a $4.3\text{ }\mu\text{m}$ BCB/I-MSM PD (same structure as described herein)/ SiO_2/Si sample had a PD dark current of less than 10 nA at 5 V , an estimated measured coupling efficiency of 21.3% , and a simulated coupling efficiency of 33.8% using scalar beam propagation method (BPM) analysis [22].

The BCB waveguide/PD/TIA structure was tested using a distributed feedback single-mode fiber-coupled laser operating at a wavelength of $1.55\text{ }\mu\text{m}$. An external modulator was used to modulate the signal, and the output of the modulator was 2 mW . The modulator single mode fiber output was endface coupled into the waveguide. The output of the PD embedded in the waveguide was $71.02\text{ }\mu\text{A}$ when the fiber was endface coupled. Fig. 6 shows the measured eye diagrams at 25 and at 100 Mbps. Both used PSRB ²⁷. Better decoupling will enable this system to operate at much higher speeds in the future.

C. Embedded PDs in Polymer Waveguides on Printed Wiring Boards

Thin-film InGaAs I-MSM PDs have also been embedded in polymer waveguide structures integrated onto high-temperature FR-4 boards [25]. A $1\text{-}\mu\text{m}$ -thick thin-film I-MSM PD was embedded into the core layer of a channel waveguide prepared on a surface planarized FR-4 printed wiring board (PWB) board. The thicknesses of core, cladding and planarizing layers were 4 , 12 , and $16\text{ }\mu\text{m}$, respectively. The PWB board needed to be planarized because the surface roughness of the board, which can cause excessive optical waveguide loss, was high. BCB was used as both the planarizing and the waveguide material. Polysiloxane (PSB-K1, Toray Industries) was used as the waveguide cladding layer. Both BCB and PSB can be cured at temperatures as low as $250\text{ }^\circ\text{C}$, which is a process temperature

consistent with high performance FR-4. The 12- μm cladding layer in the structure provided enough separation between the planarization BCB layer and core BCB layer to prevent coupling of the light signal propagating through the core from coupling into planarization layer.

The PWB used for the integration needs to have sufficient heat resistance for the waveguide integration process as well as a surface flatness sufficient for both transferring and bonding thin-film PDs and for minimizing the scattering loss of the waveguide. Several commercially available high performance PWBs were compared as candidates for integration. All of these materials were expected to have higher heat resistance than standard FR-4 due to their higher glass transition temperatures. Surface profiles of the PWBs were measured using a surface profiler (Tencor Alphastep-500) after the copper foils were removed. The measured roughness of each PWB had both a short and long period component. The short period roughness was on a 10- μm period, and was on the order of $\pm 0.5 \mu\text{m}$ for the least rough samples. The longer period roughness was on a 500- μm period, and measured $\pm 1 \mu\text{m}$ for the least rough samples. After BCB planarization, the resulting surface roughness was $\pm 0.2 \mu\text{m}$ on a 500- μm period, and the shorter period roughness could not be resolved by the profilometer measurement (resolution limitation: 2.5 nm). The sample most suited for integration was MCL-E-679F, from the Hitachi Chemical Company.

The thin-film I-MSM was integrated onto the PSB and embedded into a BCB waveguide using the same process as that used in the previous section for the Si substrates. The function of the embedded PD was tested by measuring the photocurrent and the dark current in the same manner as described in the previous section, and the output of the PD was more than 100 times larger than the I-MSM dark current. Difficulty in endface coupling from the fiber to the BCB waveguide on the PWB degraded the signal to dark current ratio, and made an estimate of the coupling efficiency difficult.

IV. PLANAR OPTICAL INTERCONNECTIONS USING EMBEDDED PERPENDICULAR BEAM TURNING DEVICES

A. 45° Beam Turning on Si Using Metal-Coated Photodielectric Epoxy Micromirrors

Optical beams can be turned from plane parallel to surface normal by using micromirrors with an angle of 45°. Using micromirrors, in-plane optical beams, from emitters or waveguides, can be turned to surface normal beams that can be launched into fibers or PDs or into free space optical systems. Critical factors to consider in mirror development include material compatibility with other materials used in an integrated system, precision and repeatability of mirror angle, reflectivity and surface quality of the reflecting surface, and the capability to mass form the mirrors in a parallel manufacturing process across a substrate or wafer.

There are a number of techniques that have been used to fabricate micromirrors. One technique that has been demonstrated is the wettability control of resin [26]. The control, reproducibility, and uniformity of this technique across large area substrates

(board size, in the multi-cm on a side range) in a parallel production mode are concerns with this method. A second method for producing micromirrors is the dynamic etch mask technique for fabricating tapered semiconductor optical waveguides and other structures [27]. Using the dynamic etch mask technique and wet chemical etchants, semiconductor structure slope angles as small as 0.9 degrees were produced. However, this technique was demonstrated only for very small structures, which had a height of 1 μm . Mirrors on the order of 100 μm in height are of interest for on-substrate integrated beam turning. This thickness of silicon dioxide is not practical from a deposition and stress standpoint, particularly over large (board-size) areas. A third technique involves the fabrication of a 45° mirror by cutting a waveguide with a 45° wedge-shaped diamond blade using a commercially available dicing saw machine which is commonly used to cut large scale integration silicon integrated circuits [28]. The small throughput using this “one sample-at-a-time” process is a significant drawback to this process.

Herein is reported for the first time a technique for producing 45° micromirrors using a photodielectric dry film epoxy material. This material has also been used to form the insulator layers in high density interconnection (HDI) substrates with embedded electrical interconnections. As reported herein, this polymer can be used to form micromirrors over a large scale using standard lamination or spin coating, UV exposure, and wet development; all processes that are used for HDI substrate fabrication, as well. The Vialux 81 polymer reported herein is used as a dielectric layer in HDI substrates with photodefined via formation over large areas (multiple cms square). Thus, the process reported herein can be used to mass form mirrors over a large substrate. To explore the repeatability of this process, 40 separately fabricated samples were created using this technique, as reported later.

A 45° mirror structure was fabricated using Vialux 81, a DuPont photodielectric epoxy dry film used to fabricate HDI electrical substrates. The epoxy dry film, when stacked, exposed to UV radiation, baked, and developed, can be engineered to form different angles and surface curvatures [29], [30]. To create a 45° mirror, two layers of 62.5- μm -thick epoxy film were laminated onto a 4-in silicon wafer. Next, the laminated wafer was diced into 0.015 cm \times 0.015 cm samples using a scribe. The samples were then exposed through a 100 μm \times 100 μm mask box pattern to 3200 mJ/cm² of UV light using a Karl Suss MJB mask aligner. After letting the sample cool for 5 min, the Mylar coversheet was removed. Next, the samples were baked for 1 h at 110 °C. After the samples cooled for another 15 min, they were developed using gamma-butyrolactone (GBL). The dwell time was 6–8 min. Next, the samples were thermally cured at 150 °C for 1 h. Since metal does not adhere well to Vialux 81, polyimide was used as an adhesion layer. Polyimide was spun onto the samples at 4000 rpm for 90 s, then cured at 350 °C for 1 h. Finally, the sample was metallized with Au to form a highly reflecting mirror surface, as shown in the cross-sectional photomicrograph in Fig. 7.

After fabricating 40 samples, the angles were measured using an Alpha-Step 500 profilometer, and these angles ranged from 40 to 50°. The sample in Fig. 7 had an angle of 45.9°. The height

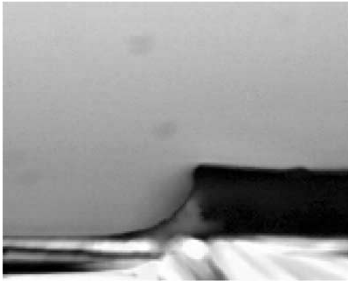


Fig. 7. Cross-sectional photomicrograph of the polymer/metal micromirror.

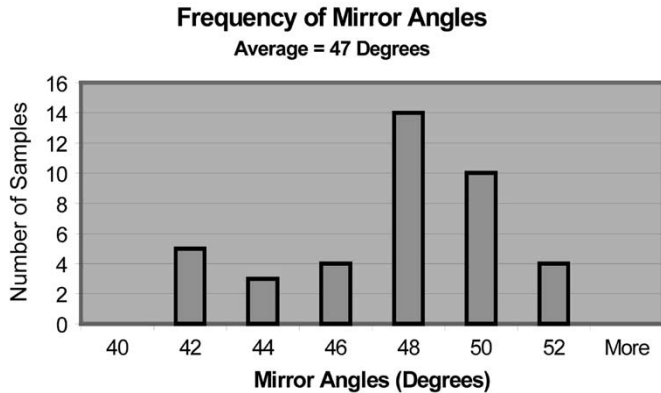


Fig. 8. Frequency distribution of the micromirror angles from 40 measured samples.

of the micromirror was $99.2 \mu\text{m}$ and the width was $96.0 \mu\text{m}$. Of the 40 samples measured, the average and median angle was 47° . The smallest angle was 41° and the largest angle was 51° . Fig. 8 is a frequency distribution of the 40 sample angles measured.

To assess the impact of the $\pm 5^\circ$ variations from 45° , a Matlab simulation of the coupling of the laser/turning mirror optical beam into a multimode optical fiber was developed. The fiber had a numerical aperture of 0.22 and a fiber core radius of $200 \mu\text{m}$. This program utilized Gaussian beam propagation for the laser light (traveling in free space) that is turned by the mirror, with an analysis of coupling into the fiber. The fiber to micromirror distance was set such that the $1/e^2$ beam slightly underfilled the micromirror. The results indicate that the variation in the mirror angle experimentally observed would have a very small effect on the amount of light accepted into the fiber: a $\pm 5^\circ$ micromirror angle variation resulted in 1.6% additional coupling loss.

B. Embedded Optical Interconnections Using Integrated Volume Gratings on Polymer Waveguides

The second type of optical beam turning device that has been studied by the authors is a volume grating coupler (VGC). VGC were fabricated and laminated onto polymer (BCB) waveguides on Si substrates, as shown schematically in Fig. 9. The output coupling efficiency of these VGCs were measured using the image capture method.

To fabricate the couplers, a laser interferometric recording configuration was used. Light from a single longitudinal mode

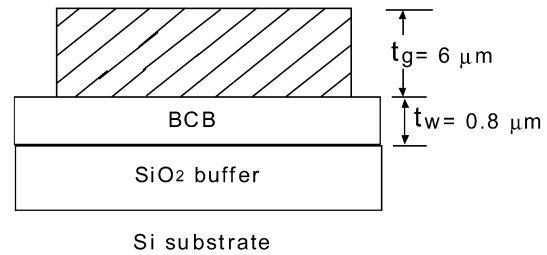


Fig. 9. Diagram of volume grating on polymer waveguide configuration.

$\lambda = 363.8 \text{ nm}$ ultraviolet (UV) laser was spatially filtered and then collimated to obtain a uniform phase front. The light was then redirected to a polarizing beamsplitter, which was preceded by a half-wave plate and followed by another half-wave plate. This configuration produced two beams whose power ratio can be accurately controlled to achieve an optimal power ratio between them. These two beams were then redirected with mirrors toward the sample being exposed. A prism was placed in front of the sample in order to achieve the angular separation required to produce a grating period and slant angle that would couple the light out vertically and achieve preferential-order coupling. Antireflection coated fused silica prisms were used for this purpose. Finally, another prism was placed behind the sample in order to minimize reflections from the sample/air interface that could affect the pattern being recorded.

The grating material used was DuPont HRF600X photopolymer, with $n_g = 1.50$ and an index modulation $\Delta n = 0.02$. The HRF600X photopolymer comes in $6\text{-}\mu\text{m}$ -thick laminate sheets sandwiched between two protective mylar layers. To produce the grating, the thinner of the two mylar cover sheets was first removed, and then the photopolymer sample was placed in between the two prisms as described earlier, with the protective mylar layer facing the back prism. For the VGC to have a straight edge, a slide with a metal mask covering a portion of it was placed against the first prism, with the sample then placed against the mask. Index matching oil was used in the prism/mask, mask/sample and sample/prism interfaces to avoid reflections. An exposure dosage of 70 mJ [31] and an exposure intensity of 0.24 mW/cm^2 [32] produce a strong index modulation in this photopolymer, and were used in these exposures. Two rubber bands, one near the bottom of the prisms and one near the top, were used to squeeze the sample between them and produce better contact between the prisms, mask, and sample. To allow for the relaxation of stresses, the exposure was not started until 2 min after the rubber bands had been placed on the sample. After exposure, the sample was rinsed with isopropanol to remove the index matching oil and then dried with nitrogen.

Once the interferometric exposure was completed, the grating layer was laminated onto the polymer waveguide. The gratings can be laminated onto the waveguides either manually with a roller, or with a laminating machine such as the HiVAC-600, by E & H Laminators. For the results reported herein, the laminating machine was utilized. After lamination, the samples were placed on a hot plate at 150°C for 20 min. Then the thin mylar layer on top of the grating was carefully peeled off, and a uniform UV exposure with $\lambda = 363 \text{ nm}$ light, with a dose of

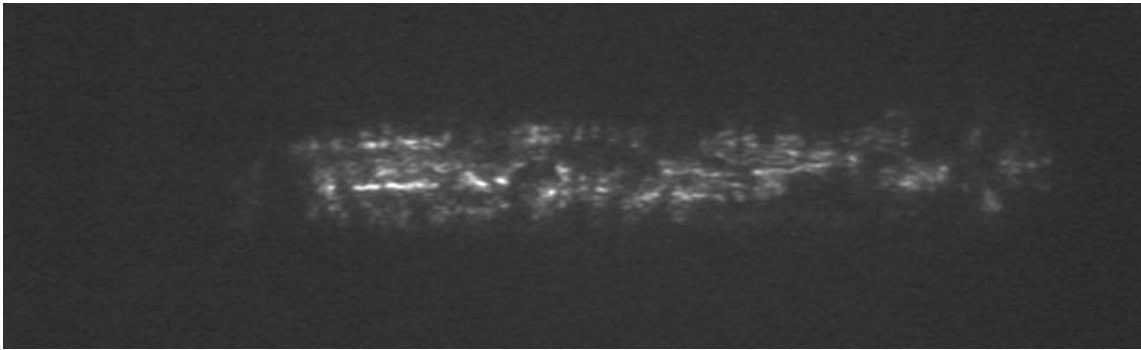


Fig. 10. Infrared (IR) image of light being coupled out of a BCB channel waveguide by a VGC laminated onto the top of the waveguide.

100 mJ, was performed on the samples. Finally, the samples were placed back on the hot plate for a final 70-min cure.

To measure the coupling efficiency of the VGCs laminated onto BCB polymer waveguides, the image capture method was used. This method is similar to the fiber scanning method described in Section III, except that the output is captured with a camera instead of a multimode fiber. A Hamamatsu model C2741-03 IR camera attached to a frame grabber was used. An image of the out-coupled light captured by this camera is shown in Fig. 10. Pixel values collected from the frame grabber were normalized and adjusted for the nonlinear response of the camera, and then an exponential fit was made to the power decay along the surface of the VGC. This decay includes the absorption and scattering losses intrinsic to the waveguide and the grating material, but these are very small compared to the effect of the coupling. The coupling coefficient is thus roughly equivalent to the exponential decay factor in the power along the surface of the coupler. The coupling coefficient was 0.56 mm^{-1} for the device shown in Fig. 10. The normalized data plot and exponential fit are shown in Fig. 11. Using this value and an estimate of 90% preferential coupling ratio (determined mainly by the geometry of the structure and thus not subject to much experimental variation), the coupling efficiency for the fabricated device, for a device $200 \mu\text{m}$ in length, was determined to be 18%.

Some of the embedded optical interconnection structures described herein have also been rigorously modeled. Three optoelectronic structures incorporating substrate-embedded InP-based inverted-MSM PDs and/or volume holographic gratings have been analyzed and compared at the primary optical communication wavelengths [33]. These structures, in conjunction with optical quality polymer layers, can be easily integrated into boards for the purpose of implementing board optical interconnections. The structures are as follows: (a) an evanescent-coupling architecture with a substrate-embedded PD; (b) a volume-holographic-grating coupler architecture with a substrate-embedded PD; and (c) a volume-holographic-grating coupler architecture with a flip-chip-bonded PD. The primary characteristic of the evanescent coupling architectures is the efficient performance for both TE and TM polarizations with the disadvantage of exponentially decreasing efficiency with increasing separation between the waveguide film layer and the PD layer. On the other hand, the primary characteristic of the volume holographic grating architectures was found to be the possibility of wavelength and polarization selectivity as well as their independence on the separation between the PD

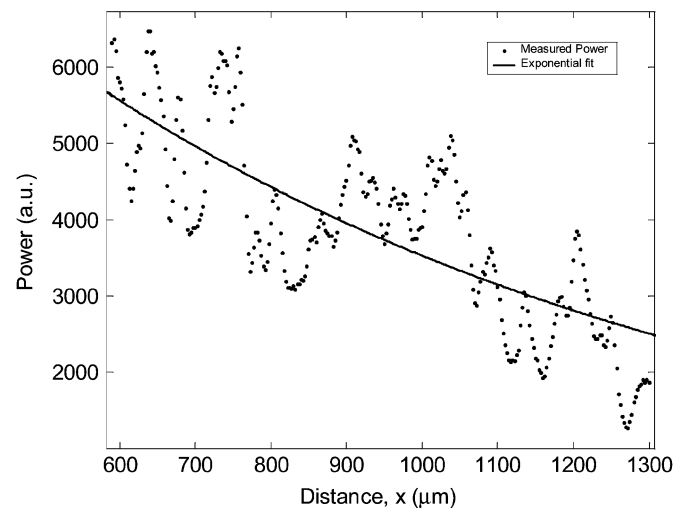


Fig. 11. Measured power along VGC surface and exponential fit.

layer and the waveguide. For the case of evanescent coupling into a substrate embedded PD, comparison of the analysis with experimental results showed good agreement [33].

V. CONCLUSION

Planar optical interconnections integrated onto boards to realize embedded optical interconnections have been discussed herein from a design, fabrication, test, and theoretical perspective. Options for both beam turning and embedded interconnections to active optoelectronic devices, have been discussed. Integration processes for creating embedded planar optical interconnections have been described, and measurement results for a number of integration schemes that have been demonstrated by the authors were presented. In the area of optical interconnections with beams coupled to and from the board, the topics covered include integrated metal-coated polymer mirrors and volume holographic gratings for optical beam turning perpendicular to the board. Optical interconnections that utilize active thin-film optoelectronic components embedded in the board were also discussed, using both Si and high temperature FR-4 substrates. While the results in this paper discuss advanced integration technology, and hence, report speeds only up to 100 Mbps, other papers on this topic report data rates much higher, including 16.75 ps FWHM for a thin-film PD embedded in a waveguide [22] and 4.8 ps FWHM for a $40\text{-}\mu\text{m}$ -diameter thin-film PD integrated onto a Si substrate [34]. Thus,

as data rates increase and board-level interconnections become system-limiting performance factors, board-level embedded optical interconnections are becoming viable alternative interconnection technologies.

ACKNOWLEDGMENT

The authors would like to acknowledge the staff of the Georgia Tech Microelectronics Research Center cleanroom for their support.

REFERENCES

- [1] E. D. Kyriakis-Bitzaros, N. Haralabidis, M. Lagadas, A. Georgakilas, Y. Moisiadis, and G. Halkias, "Realistic end-to-end simulation of the optoelectronic links and comparison with the electrical interconnections for system-on-chip applications," *J. Lightwave Technol.*, vol. 19, pp. 1532–1542, 2001.
- [2] W. Ryu, J. Lee, H. Kim, S. Ahn, N. Kim, B. Choi, D. Kam, and J. Kim, "RF interconnect for multi-Gbit/s board-level clock distribution," *IEEE Trans. Adv. Packag.*, vol. 23, pp. 398–407, 2000.
- [3] D. A. B. Miller, "Rationale and challenges for optical interconnects to electronic chips," *Proc. IEEE*, vol. 88, pp. 728–749, 2000.
- [4] S. K. Tewksbury and L. A. Hornak, "Optical clock distribution in electronic systems," in *J. VLSI Signal Process.*, vol. 16, 1997, pp. 225–246.
- [5] M. Rassaian and M. W. Beranek, "Quantitative characterization of 96.5Sn3.5Ag and 80Au20Sn optical fiber solder bond joints on silicon micro-optical bench substrates," *IEEE Trans. Adv. Packag.*, vol. 22, pp. 86–93, 1999.
- [6] S. J. Walker and J. Jahns, "Optical clock distribution using integrated free-space optics," *Opt. Commun.*, vol. 90, pp. 359–371, 1992.
- [7] P. J. Delfyett, D. H. Hartman, and S. Z. Ahmad, "Optical clock distribution using a mode-locked semiconductor laser-diode system," *J. Lightwave Technol.*, vol. 9, pp. 1646–1649, 1991.
- [8] Y. Liu, L. Lin, C. Choi, B. Bihari, and R. T. Chen, "Optoelectronic integration of polymer waveguide array and metal—Semiconductor-metal photodetector through micromirror couplers," *IEEE Photon. Technol. Lett.*, vol. 13, pp. 355–357, 2001.
- [9] S. M. Schultz, E. N. Glytsis, and T. K. Gaylord, "Volume grating preferential-order focusing waveguide coupler," *Opt. Lett.*, vol. 24, pp. 1708–1710, 1999.
- [10] N. M. Jokerst, M. A. Brooke, J. Laskar, D. Scott Wills, A. S. Brown, M. Vrazel, S. Jung, Y. Joo, and J. J. Chang, "Microsystem optoelectronic integration for mixed multisignal systems," *IEEE J. Select. Top. Quantum Electron.*, vol. 6, pp. 1231–1239, 2000.
- [11] St. Kollakowski, A. Strittmatter, E. Dröge, E. H. Böttcher, and D. Bimberg, "65 GHz InGaAs/InAlGaAs/InP waveguide-integrated photodetectors for the 1.3–1.55 μm wavelength regime," *Appl. Phys. Lett.*, vol. 74, pp. 612–614, 1999.
- [12] E. H. Böttcher, H. Pfitzenmaier, E. Dröge, St. Kollakowski, A. Strittmatter, D. Bimberg, and R. Steingrüber, "Distributed waveguide-integrated InGaAs MSM Photodetectors for high-efficiency and ultra-wideband operation," in *Proc. IEEE 11th Int. Conf. Indium Phosphide and Related Mater.*, 1999, pp. 79–82.
- [13] R. T. Chen, L. Lin, C. C. Choi, Y. J. Liu, B. Bihari, L. Wu, S. Tang, R. Wickman, B. Picor, M. K. Hibbs-Brenner, J. Bristow, and Y. S. Liu, "Fully embedded board-level guided-wave optoelectronic interconnects," *Proc. IEEE*, vol. 88, pp. 780–793, 2000.
- [14] C. H. Buchal, A. Roelofs, M. Siegert, and M. Löken, "Polymeric strip waveguides and their connection to very thin ultrafast metal-semiconductor-metal detectors," in *Mater. Res. Soc. Symp. Proc.*, vol. 597, 2000, pp. 97–102.
- [15] F. Gouin, L. Robitaille, C. L. Callender, J. Noad, and C. Almeida, "A 4×4 optoelectronic switch matrix integrating an MSM array with polyimide optical waveguides," *SPIE*, vol. 3290, pp. 287–295, 1997.
- [16] H. Kuo, S. Cho, J. Hall, and N. Jokerst, "InP/InGaAsP MQW thin film edge emitting lasers for embedded waveguide chip to chip optical interconnections," *Proc. 16th Annual Meeting IEEE LEOS*, vol. MG2, pp. 63–64, 2003.
- [17] Y. Ohiso, H. Okamoto, R. Iga, K. Kishi, K. Tatenno, and C. Amano, "1.55- μm buried-heterostructure VCSEL's with InGaAsP/InP-GaAs/AlAs DBR's on a GaAs substrate," *IEEE J. Quantum Electron.*, vol. 37, pp. 1194–1202, Sept. 2001.
- [18] S. Cho, J. Hall, A. Chellappa, N. Jokerst, and M. Brooke, "High speed optical interconnection using embedded PD's on electrical boards," in *Proc. 53rd Electronic Components and Technology Conf.*, New Orleans, LA, 2003, pp. 1046–1052.
- [19] D. G. Ivey, P. Jian, R. Bruce, and G. Knight, "Microstructural analysis of Au/Pt/Ti contacts to p-type InGaAs," *J. Mater. Sci.: Mater. in Electron.*, vol. 6, pp. 219–227, 1995.
- [20] N. M. Jokerst, M. Brooke, S. Y. Cho, S. Wilkinson, M. Vrazel, S. Fike, J. Tabler, Y. J. Joo, S. W. Seo, D. S. Wills, and A. Brown, "The heterogeneous integration of optical interconnections into integrated microsystems," *IEEE J. Select. Topics Quantum Electron.*, vol. 9, pp. 350–360, Mar./Apr. 2003.
- [21] Hitachi Chemical. Personal correspondence with N. Ogawa.
- [22] S. Cho, M. Brook, and N. Jokerst, "Optical interconnections on electrical boards using embedded active optoelectronic components," *IEEE J. Select. Topics Quantum Electron.*, pp. 465–476, Mar./Apr. 2003.
- [23] S. Wolff, A. R. Giehl, M. Renno, and H. Fouckhardt, "Metallic waveguide mirrors in polymer film waveguides," *Appl. Phys. B*, vol. 73, pp. 623–627, 2001.
- [24] G. Fischbeck, R. Moosburger, M. Topper, and K. Peterman, "Design concept for singlemode polymer waveguides," *Electron. Lett.*, vol. 32, pp. 212–213, 1996.
- [25] T. Suzuki, T. Nonaka, S. Cho, N. Jokerst, and R. Tummala, "Embedded optical interconnections on printed wiring boards," in *Proc. 53rd Electronic Components and Technology Conf.*, New Orleans, LA, 2003, pp. 1153–1159.
- [26] H. Teriu and K. Shutoh, "Novel micromirror for vertical optical path conversion formed in silica-based PLC using wettability control of resin," *J. Lightwave Technol.*, vol. 16, pp. 1631–1639, 1998.
- [27] A. Shahar, W. J. Tomlinson, A. Yi-Yan, M. Seto, and R. J. Deri, "Dynamic etch mask technique for fabricating tapered semiconductor optical waveguides and other structures," *Appl. Phys. Lett.*, vol. 56, no. 12, pp. 1098–1100, 1990.
- [28] R. Yoshimura, M. Hikita, and S. Imamura, "Low-loss polymeric optical waveguides with 45° mirrors," *Jpn. J. Appl. Phys.*, pt. 1, vol. 37, no. 6B, pp. 3657–3661, 1998.
- [29] N. White. (2001) *Aqueous Dry Film Development* [Online]. Available: <http://www.dupont.com/pcm/techinfo/develop/develop4.pdf>
- [30] C. Gonzalez, "High-impact spraying for photoresist processing," *Printed Circuit Fabr.*, vol. 10, no. 5, pp. 51–54, 1987.
- [31] S. M. Schultz, "High efficiency volume grating coupler," Ph.D. dissertation, Georgia Inst. Technol., Atlanta, 1999.
- [32] S. D. Wu and E. N. Glytsis, "Holographic grating formation in photopolymers: Analysis and experimental results based on a nonlocal diffusion model and the rigorous coupled-wave analysis," *J. Opt. Soc. Amer. B*, vol. 20, pp. 3046–3052, June 2003.
- [33] E. N. Glytsis, N. M. Jokerst, R. A. Villalaz, S. Y. Cho, S. D. Wu, Z. Huang, M. A. Brooke, and T. K. Gaylord, "Substrate-embedded and flip-chip-bonded photodetector polymer-based optical interconnects: Analysis, design, and performance," *J. Lightwave Technol.*, vol. 20, pp. 2382–2394, Oct. 2003.
- [34] S. W. Seo, J. J. Shen, N. M. Jokerst, and A. S. Brown, "Heterogeneous integrated large area, high speed InGaAs thin film metal-semiconductor-metal photodetectors for integrated optoelectronics," in *IEEE Proc. Conf. Lasers and Electro-Opt.*, June 2003. TuD3.



Nan M. Jokerst (F'03) received the Ph.D. degree from the University of Southern California, Los Angeles, in 1989.

She is currently the J. A. Jones Distinguished Professor in the School of Electrical and Computer Engineering, Duke University, Durham, NC. She joined the Electrical and Computer Engineering faculty of Duke University in 2003 after 15 years as a faculty member of the Georgia Institute of Technology, Atlanta. She has published and presented more than 200 papers, three book chapters, and has four patents awarded and one pending.

Dr. Jokerst received the IEEE Education Society/Hewlett Packard Harriet B. Rigas Award (2002), an IEEE Millennium Medal (2000), and is a Fellow of the Optical Society of America (2000). She is a DuPont Young Faculty Award winner and a National Science Foundation Presidential Young Investigator. She won a Newport Research Award, three teaching awards, and was a Hewlett Packard Fellow. She has organized and served on numerous conference committees, and served on the Board of Directors of the Optical Society of America as the Chair of the Engineering Council, also on the IEEE Lasers and Electro-Optic Society (LEOS) Board of Governors as an elected member, and as the Vice President of Conferences for IEEE LEOS. She has also served as the elected Chair, Vice Chair, Secretary, and Treasurer of the Atlanta IEEE Section.



Thomas K. Gaylord (S'65–M'70–SM'77–F'83) received the B.S. and M.S. degrees in physics and electrical engineering, respectively, from the University of Missouri-Rolla and the Ph.D. degree in electrical engineering from Rice University, Houston, TX.

Currently, he is with the Georgia Institute of Technology (Georgia Tech), Atlanta, where he is the Julius Brown Chair and Regents' Professor of Electrical and Computer Engineering. He is the author of approximately 350 technical publications and 25 patents in the areas of diffractive optics, optoelectronics, and semiconductor devices.

Dr. Gaylord received the "Curtis W. McGraw Research Award" from the American Society for Engineering Education; the IEEE Centennial Medal; the IEEE Graduate Teaching Award; and the Georgia Tech Outstanding Teacher.



Demetris L. Geddis (M'97) received the B.S. degree in electrical engineering from Hampton University, Hampton, VA, and the M.S. and Ph.D. degrees, both in electrical and computer engineering, from the Georgia Institute of Technology, Atlanta.

He has extensive research experience in the areas of integrated optoelectronics, optics, microelectronics, and electromagnetics. He has worked as a Research and Design engineer with Motorola and Bell Laboratories. Current research interests and publications are in the areas of photonics, optoelectronics, microelectronics, heterogeneous thin-film integration, and single-fiber bidirectional communications. In 2004, he joined Norfolk State University, Norfolk, VA, as an Assistant Professor of optical engineering.

Dr. Geddis is a Member of the IEEE Lasers and Electro-Optic Society.

E. Glytsis (S'81–M'86–SM'91), photograph and biography not available at the time of publication.

Martin A. Brooke (S'85–M'87), photograph and biography not available at the time of publication.



Jaemin Shin was born in Seoul, Korea, on December 18, 1973. He received the B.S. degree in control and instrumentation engineering from Korea University, Korea, in 1998, and the M.S. degree in 2003 from the Georgia Institute of Technology (Georgia Tech), Atlanta.

He is currently pursuing the Ph.D. degree under Dr. Brooke's advice in electrical and computer engineering at Georgia Tech. He has two years of industrial experience with an optical fiber manufacturing company in Korea. His research interest is in the development of optical interconnect with optical waveguide, comparison of optical interconnect with electrical interconnect, and modeling for high-frequency interconnect on low-cost substrate.

development of optical interconnect with optical waveguide, comparison of optical interconnect with electrical interconnect, and modeling for high-frequency interconnect on low-cost substrate.

R. Villalaz, photograph and biography not available at the time of publication.

J. Hall, photograph and biography not available at the time of publication.



S. Cho (M'03) received the Ph.D. degree from the Georgia Institute of Technology, Atlanta, in 2003.

He is currently a research engineer with Duke University, Durham, NC. His research interests include board-level high-speed optical interconnections, integrated photonic biochemical sensors, and ultrahigh-speed wavelength converters in WDM system.



Toshihisa Nonaka received the B.S. degree in industrial chemistry from the University of Tokyo, Tokyo, Japan, in 1986 and the Ph.D. degree from Nagoya University, Japan, in 1995.

He has been with Toray Industries, Inc. since 1986. He was a visiting scholar with the Packaging Research Center, Georgia Institute of Technology, Atlanta, from 2001 to 2003. He is currently working on the material development for microsystem packaging including optical interconnection.



Ananthasayanam Chellappa received the B.Tech. degree from the Indian Institute of Technology, Madras, in 1998.

He then joined Texas Instruments (India) for a while where he designed catalog and application-specific data converters and PLLs for flat panel display transceivers. In 2001, he joined the Georgia Institute of Technology, Atlanta. He has been involved in the design of optical receivers and is currently working on low-area high-speed receivers applicable to chip-to-chip optical interconnect.

He also has interests in design automation and robotics.

T. Suzuki, photograph and biography not available at the time of publication.

M. Vrazel, photograph and biography not available at the time of publication.